

Analysis of Th-U breeding capability for an accelerator-driven subcritical molten salt reactor

Xue-Chao Zhao^{1,2,3} · De-Yang Cui^{1,2,3} · Xiang-Zhou Cai^{1,2,3} · Jin-Gen Chen^{1,2,3}

Received: 13 March 2018 / Revised: 19 April 2018 / Accepted: 7 May 2018 / Published online: 9 July 2018

© Shanghai Institute of Applied Physics, Chinese Academy of Sciences, Chinese Nuclear Society, Science Press China and Springer Nature Singapore Pte Ltd. 2018

Abstract Accelerator-driven systems based on molten salt fuel have several unique advantages and features for advanced nuclear fuel utilization. The aim of this work was to study the Th-U breeding capability in such systems, known as “accelerator-driven subcritical molten salt reactors” (ADS-MSRs). Breeding capacities including conversion ratio and net ²³³U production for various subcriticalities and different minor actinides (MA) loadings were analyzed for an ADS-MSR. The results show that the subcriticality of the core has a considerable effect on the Th-U breeding. A high subcriticality is favorable to improving the conversion ratio, increasing the net ²³³U production, and reducing the doubling time. Specifically, the doubling time for k_{eff} of 0.99 is larger than 80 years, while the counterpart for k_{eff} of 0.93 is only approximately 22 years. Nevertheless, in an ADS-MSR with a high initial

MA loading, MA results in a non-negligible ²³³U depletion in the first two decades, while increasing the net ²³³U production compared to reactors without MA loading. During the 50 years of operation, for the subcritical reactor ($k_{\text{eff}} = 0.97$) with MA fraction increasing from 1 to 14%, the net ²³³U production increases from 3.94 to 8.24 t.

Keywords Subcritical · Molten salt fuel · Conversion ratio · Net ²³³U production

1 Introduction

Accelerator-driven subcritical systems (ADS), which were originally proposed as power amplifiers, attract increasing attention in the field of nuclear waste transmutation and thorium resource utilization, owing to their inherent safety with external neutron sources and subcritical characteristics [1, 2]. Under subcritical conditions, the operation of these kinds of systems depends on the external neutrons generated from spallation reactions by the collision of high-energy protons and a heavy metal target. Owing to the benefits of the subcritical characteristics ADS have higher safety than traditional critical reactors. This higher safety performance allows a higher minor actinides (MA) loading; thus, the accelerator-driven subcritical system is very flexible for spent fuel incineration [3]. Although most of the ADS designs are based on traditional solid fuel, molten salt fuel can be considered as an alternative and attractive option for the subcritical reactor. As one of the six candidate reactors chosen by the Generation IV International Forum (GIF), molten salt reactors (MSRs) have several outstanding advantages in advanced nuclear

This work was supported by the Chinese TMSR Strategic Pioneer Science and Technology Project (No. XDA02010000) and the Frontier Science Key Program of the Chinese Academy of Sciences (No. QYZDY-SSW-JSC016).

✉ Xiang-Zhou Cai
caixz@sinap.ac.cn

✉ Jin-Gen Chen
chenjg@sinap.ac.cn

Xue-Chao Zhao
zhaoxuechao@sinap.ac.cn

¹ Shanghai Institute of Applied Physics, Chinese Academy of Sciences, Shanghai 201800, China

² CAS Innovative Academies in TMSR Energy System, Chinese Academy of Sciences, Shanghai 201800, China

³ University of Chinese Academy of Sciences, Beijing 100049, China

fuel utilization as well [4–7]. Compared to traditional solid fuel reactors, the application of molten salt fuel enables a relatively easy online fuel processing, subsequently achieving significantly high neutron economics and fuel utilization. Combining the characteristics of the ADS and the MSR, the accelerator-driven subcritical molten salt reactor (ADS–MSR) has certain specific advantages and features. The power distribution in the core can become flat due to a high heat capacity and excellent thermal conductivity of the molten salt fuel, while the radiation damage of the fuel assembly can be mitigated. With online fuel feeding, the stable operation (k_{eff}) of the reactor can be maintained conveniently, which is beneficial to the long-term stability of the subcritical reactor.

Several ADS concepts based on molten salt fuel have been proposed since the late 1980s. Most of these designs are optimized for both power production and transuranic (TRU) transmutation. Furukawa et al. developed the conceptual design of the thorium molten salt nuclear energy synergetic system (THORIMS-NES) [8]. An accelerator molten salt breeder (AMSB) was proposed for fissile fuel production for the THORIMS-NES [9]. The French Alternative Energies and Atomic Energy Commission (CEA) proposed a concept of a thorium-fueled ADSR, called “TASSE” [10], for TRU burning with power production. Bowman et al. proposed different types of molten salt reactors for the accelerator-driven transmutation of waste (ATW) for incinerating plutonium and to prevent nuclear proliferation in the early 1990s. The Tier 1–Tier 2 molten salt systems by Bowman [11] were designed to transmute TRU from the spent fuel without advanced spent fuel reprocessing. The Tier 1 system is a once-through transmuter based on NaF–ZrF₄, while the Tier 2 system is a final actinide burner based on LiF–BeF₂. The actinides molten salt transmuter (AMSTER) [12], proposed by Vergnes et al., uses the same salt composition as the molten salt breeder reactor (MSBR) designed by the Oak Ridge National Laboratory (ORNL), and its aim is to burn TRUs with uranium or thorium. It can be considered as the revised version of the MSBR but designed for TRU incineration instead of fuel breeding. The Kurchatov Institute proposed a design of a cascade subcritical molten salt reactor (CSMSR) to burn TRU [13, 14], in which the core is divided into thermal and fast neutron zones. The aim of the cascade scheme of the subcritical reactor is to eliminate the need for an accelerator proton beam.

In this paper, the Th–U breeding capacities are assessed for various subcriticalities and different initial MA loadings in an accelerator-driven subcritical molten salt reactor. The reactor in this study was based on the ²³²Th–²³³U fuel cycle, and online refueling and fuel reprocessing were used to reduce the neutron absorption in the fission products

(FPs) and to control subcriticality. Section 2 describes the core and the simulation tools, while Sect. 3 presents the results and discussion. In Sect. 4, the conclusions are given.

2 Methodology

2.1 Reactor description and modeling

A schematic of the core of the ADS–MSR is shown in Fig. 1. The core was composed of a subcritical cladding and a liquid lead–bismuth alloy spallation target. The subcritical reactor core was cylindrical, and no graphite moderator was used in order to improve the neutron economy. A unique characteristic of the ADS–MSR is that, compared to sodium/lead cooled fast reactors, there is no traditional fuel subassembly in the reactor. The fuel was liquid fluoride salt, which was also used as primary circuit coolant. The heavy nuclides (HN) in the fuel salt comprised of ²³³U and ²³²Th, while only ²³²Th was loaded in the fertile salt. The total fuel salt volume was 12 m³, of which approximately one half was inside the active zone and the other half was outside the core. A radial reflector with a thickness of 50 cm was employed to decrease the

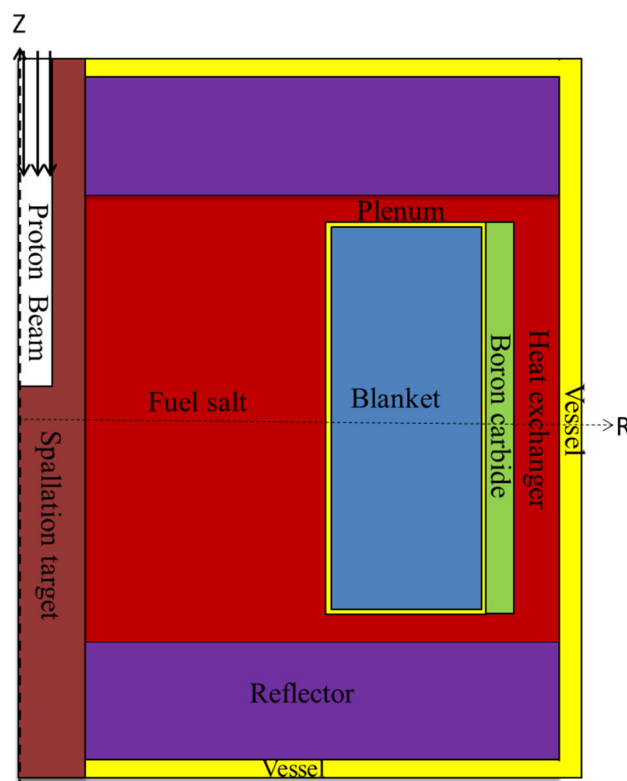


Fig. 1 Geometrical description of the symmetrical half core of the reactor

leakage of the neutrons. A 10-cm-thick B₄C neutron protection layer was placed outside the reflector. The main parameters of the subcritical reactor are summarized in Table 1. The lead–bismuth alloy spallation target was placed at the center of the core. In most the cases, a proton accelerator power was required to achieve an intensity of several tens of milliamperes, depending on the thermal power and the energy amplification coefficient of the reactor. The proton energy was set to 1 GeV, which was proven to be sufficient to obtain a high spallation neutron production. A high-energy proton beam, generated in the accelerator, was shot into the spallation target from the upper pipe, resulting in a spallation reaction with the target, which generated a mass of spallation neutrons to maintain the operation of the subcritical system.

An important advantage of the molten salt reactor is that it is relatively easy for liquid salt to implement the online processing. During the operation of the reactor, the reactor core inevitably accumulates large amounts of neutron poisons, which reach an equilibrium mass value over time. The regular separating and removing of these neutron poisons can reduce the invalid neutron absorption and improve core neutron economy, allowing more surplus neutrons for waste transmutation or fuel breeding. The primary aim of online fuel processing is to extract the fission products, while the actinides nuclide can be returned to the core at the same time. The processing units can mainly be divided into two different parts: the bubbling system and the pyro-chemical system. The bubbling system is used to separate the non-soluble gaseous and metal FPs. The electrochemical unit is used to separate and extract actinides nuclide, lanthanide nuclide, and other fission products. The removal period of non-soluble gaseous and metal FPs was set to 30 s, while the period of other FPs were assumed to be 180 days.

Table 1 Main parameters for the ADS-MSR

Parameter	Value
k_{eff}	< 1
Thermal power (MWth)	2000
Proton energy (GeV)	1
Spallation target	Liquid Pb–Bi
Fuel composition (mol fraction %)	77.5Li-22.5HNF ₄
Fuel salt volume (m ³)	12
Fuel salt volume in active zone (m ³)	6
Li7 enrichment (mol%)	99.995
Fertile salt volume (m ³)	5.65
Reactor temperature (K)	1000

2.2 Calculation tool

In this work, the geometrical and particle transport characteristics of the lead–bismuth target were simulated by the Monte Carlo N-Particle eXtended transport code-MCNPX 2.6.0 [15], which is able to trace several particles, including neutrons and protons. Then, the MCNP5 code was used for the neutron transportation calculation of the subcritical core, with the spallation neutrons calculated from MCNPX as the input source, simulating the neutron reaction process after the spallation neutrons entering the fuel salt. Finally, the burnup calculation was completed by combining MCNP5 and ORIGEN2.0 codes with the ENDF/B-VII library [16].

3 Results and discussion

3.1 Conversion ratio and ²³³U production for subcriticality

In this work, to assess the breeding capability of the subcritical Th-²³³U molten salt reactor, the conversion ratios (CRs) for different subcriticalities ($k_{\text{eff}} = 0.99/0.97/0.95/0.93$) were calculated. The CR reflects the breeding capability of fissile materials in the reactor, which can be expressed as

$$\text{CR} = \frac{R_c(^{232}\text{Th} + ^{234}\text{U} + ^{238}\text{U} + ^{240}\text{Pu} - ^{233}\text{Pa})}{R_a(^{233}\text{U} + ^{235}\text{U} + ^{239}\text{Pu} + ^{241}\text{Pu})}, \quad (1)$$

where the number R_c represents the capture reaction rates of fertile nuclides, while R_a denotes the absorption reaction rates of the fissile nuclides.

At the beginning of the burnup, only ²³³U and ²³²Th were loaded in the reactor. The variation of CR mainly depends on the initial mass ratio of ²³³U/²³²Th. In this work, the initial ²³³U loadings were 3.53, 3.41, 3.27, and 3.16 t with the corresponding initial CRs of 1.076, 1.113, 1.163, and 1.203, respectively, for different subcriticalities ($k_{\text{eff}} = 0.99/0.97/0.95/0.93$). The reactor with a deeper subcriticality requires a lower mass ratio of ²³³U/²³²Th, resulting in a higher $R_c(^{232}\text{Th})/R_a(^{233}\text{U})$ and a higher CR.

Equation (1) defines CR based on the fission and absorption rates of fissile and fertile fuel without considering the effect of the separation of spallation neutrons on the CR. In order to further understand the CR from a different perspective, it was analyzed with respect to the neutron balance. For fissile fuel, the number of absorbed neutrons per fission is $1 + \alpha$, where α is the capture-to-fission ratio. In addition to the neutron losses and captures in the structural material (v_m), the number of available neutrons for regeneration and breeding of nuclear fuel is

$v_c = v - (1 + \alpha) - v_m$. For a subcritical reactor, the number of additional spallation neutrons can be expressed as $v_s = ((1 - k)/k)v$. Then, the CR for a subcritical reactor can be defined as:

$$CR = \frac{v - (1 + \alpha) - v_m + v_s}{1 + \alpha} \tag{2}$$

Equation (2) above describes the effect of various parameters on the CR more directly. In a critical reactor, the main approaches to improve the CR are design optimizations based on v_m , v and α , which depend on the reactor size, structure material, and nuclear fuel, while the design margin is very small for a reactor with a specific neutron spectra and fuel cycle. For a subcritical reactor, it is relatively more flexible to improve CR by regulating the subcriticality. The spallation neutron numbers v_s are 0.025, 0.077, 0.132, 0.188 for different subcriticalities ($k_{eff} = 0.99/ 0.97/ 0.95/ 0.93$) and the CR increase nearly linearly with the increasing v_s . However, a trade-off needs to be made between the higher conversion ratio and the increasing need to apply an accelerator proton beam.

The nuclear fuel breeding capacity is considered excellent especially in a subcritical reactor using the molten salt fuel, which has the important advantage of online refueling. During the operation of the reactor, ^{233}U and ^{232}Th can be fed into the core to ensure the reactor steady-state operation, avoiding reactivity fluctuation resulting from the breeding/depletion of the initial nuclear fuel and the accumulation of FPs. The online refueling strategy not only simplifies the reactor control requirements but also suppresses the excess reactivity, which decreases the required initial fissile fuel inventory. In addition, ^{233}Pa can also be extracted from the fuel salt to decay into ^{233}U to decrease the absorption of ^{233}Pa and increase ^{233}U production. Variations of k_{eff} with the burnup for different subcriticalities are shown in Fig. 2. It can be seen, that with

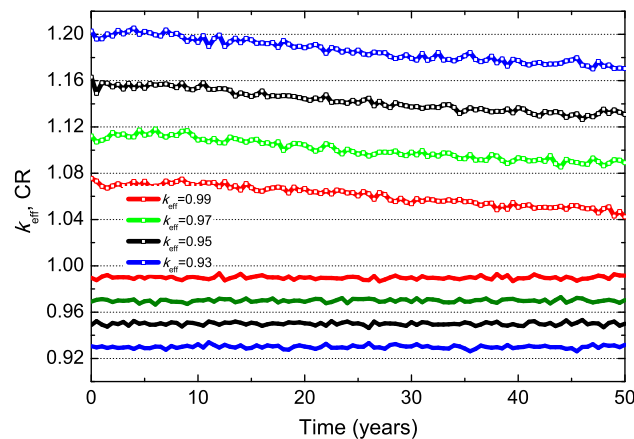


Fig. 2 Time evolution of k_{eff} (solid lines) and CR (open lines) (Color online)

online fuel processing and refueling, the k_{eff} stability at the different subcritical conditions can be maintained during the entire cycle.

Figure 2 shows the time evolution of CR with the burnup for different subcriticalities. The CR slightly declines in the evolution period of 50 years, which mainly results from the accumulation of actinides, such as plutonium and other uranium isotopes, as shown in Fig. 3. The capture-to-fission ratios (α) of ^{235}U , ^{239}Pu and ^{241}Pu under this neutron spectra are about 0.36, 0.50, and 0.22, respectively, while the α of ^{233}U is about 0.149. This indicates that ^{233}U has a better neutronic performance for breeding. The inventories of these generated ^{235}U and ^{239}Pu increase with the time of the burnup, leading to a decline of the fissile fraction of ^{233}U from 100 to about 92% and resulting in the decrease of the CR.

The net ^{233}U production can be calculated by the difference of the initial ^{233}U loading at the beginning of burnup and the ^{233}U inventories at the end of burnup. For a subcritical molten salt reactor with online fuel processing and refueling, most of the regenerative ^{233}U originates from ^{233}Pa decays outside the core. Some of ^{233}U were fed back into the core to control the reactivity, and the excess ^{233}U as a net production can be stored outside the core or used for other reactors. The amount fed ^{233}U and the extracted ^{233}Pa needs to be included in the calculation of the breeding of ^{233}U as well. The actual ^{233}U production can be expressed as

$$^{233}\text{U}(\text{production}) = ^{233}\text{U}(\text{residual}) + ^{233}\text{Pa}(\text{extract}) - ^{233}\text{U}(\text{injected}), \tag{3}$$

where ^{233}U (residual) refers to the residual ^{233}U inventory in the fuel and fertile salt, ^{233}Pa (extract) refers to the ^{233}Pa

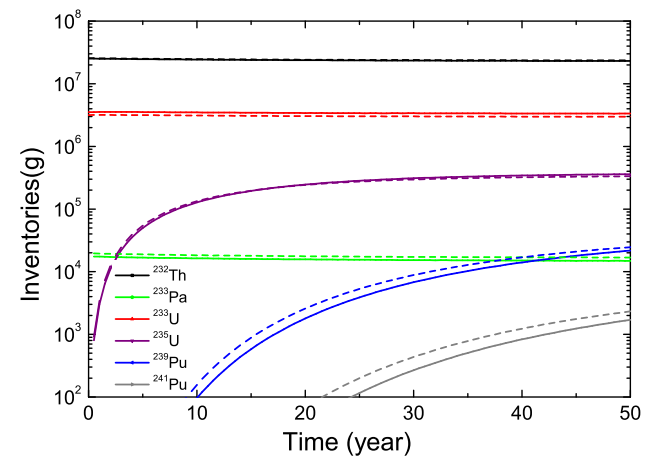


Fig. 3 Time evolution of actinides inventories for $k_{eff} = 0.99$ (solid lines) and $k_{eff} = 0.93$ (dashed lines) (Color online)

extracted from the fuel and fertile salt, ^{233}U (injected) refers to the initial and online ^{233}U feeding to the fuel salt.

Figure 4 shows the net ^{233}U production during the time of operation for different subcriticalities. It can be seen, that a high subcriticality has a considerable effect on the ^{233}U production. The doubling time for k_{eff} of 0.99 is larger than 80 years, while the counterpart for k_{eff} of 0.93 is only about 22 years. The ^{233}U breeding is closely related to CR, which mainly depends on the inventory mass ratio of $^{232}\text{Th}/^{233}\text{U}$ in the reactor. From the view of fuel processing and refueling, ^{233}Pa extraction and ^{233}U feeding are factors directly affecting the net ^{233}U production. When $k_{\text{eff}} = 0.93$, more ^{233}Pa is extracted continuously and placed outside the core to decay into ^{233}U due to the higher absorption reaction rate of ^{232}Th . Meanwhile, fewer ^{233}U needs to be fed back into the core due to the higher subcriticality. Therefore, the accumulation of excess ^{233}U outside the core as a net production is higher than that in the reactor of $k_{\text{eff}} = 0.99$.

3.2 Reactivity for MA Loading

In a subcritical system, the higher safety performance allows higher MA loading; thus, it is very flexible for MA transmutation. Meanwhile, MA are expected to show better neutronic performance in reactors with a fast neutron spectrum. When proportional MA are loaded into the fuel salt, it is necessary to analyze the ^{233}U breeding capability in the subcritical molten salt reactor. In this work, MA were recovered from the spent nuclear fuel of a pressurized water reactor (PWR) with a burnup of 33 GWd/t following a 3-year cooling period [17], with the weight ratios for ^{237}Np , ^{241}Am , ^{243}Am , ^{243}Cm , ^{244}Cm , and ^{245}Cm of 56.2, 26.4, 12.0, 0.03, 5.11, and 0.26%, respectively. For the fuel salt $77.5\text{LiF}-22.5\text{HNF}_4$, we assumed that the compositions

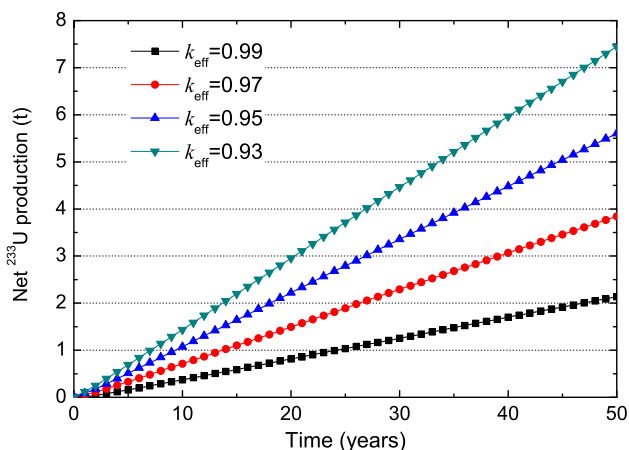


Fig. 4 Time evolution of net ^{233}U production as a function of subcriticality (Color online)

of actinides were not affecting the solubility strongly. For the selection of k_{eff} both the safety margin and energy gain were considered. For the low subcriticality case ($k_{\text{eff}} > 0.98$), the introduction of a small amount of positive reactivity results in a significant increase of neutron flux and thermal power, and an additional shutdown protection system is required. Nevertheless, $k_{\text{eff}} < 0.95$ can eliminate the need for shutdown protection systems and has a greater safety margin with respect to the insertion of reactivity; however, it reduces the system energy gain and increases the demand for accelerator power. Thus, in this section, $k_{\text{eff}} = 0.97$ is supposed to better for research purposes .

Figure 5a shows the required initial actinides loading as a function of MA fraction for $k_{\text{eff}} = 0.97$. It can be seen that the ^{232}Th inventory decreases nearly linearly with the increasing MA fraction, and the ^{232}Th inventory is not required as the MA fraction reaches 19.1%. In addition, the ^{233}U loading mass increases with the increasing MA fraction, reaches a peak value at about MA = 9%, and then decreases. This results from the change of the cross section of the actinides fission/capture for different MA loadings. Figure 5b shows the various fission rate fractions of the main heavy nuclides (^{233}U , MA and ^{232}Th) for different MA loadings at the beginning of the burnup. It can be seen, that when the MA loading varies in the range of 0–19.1%,

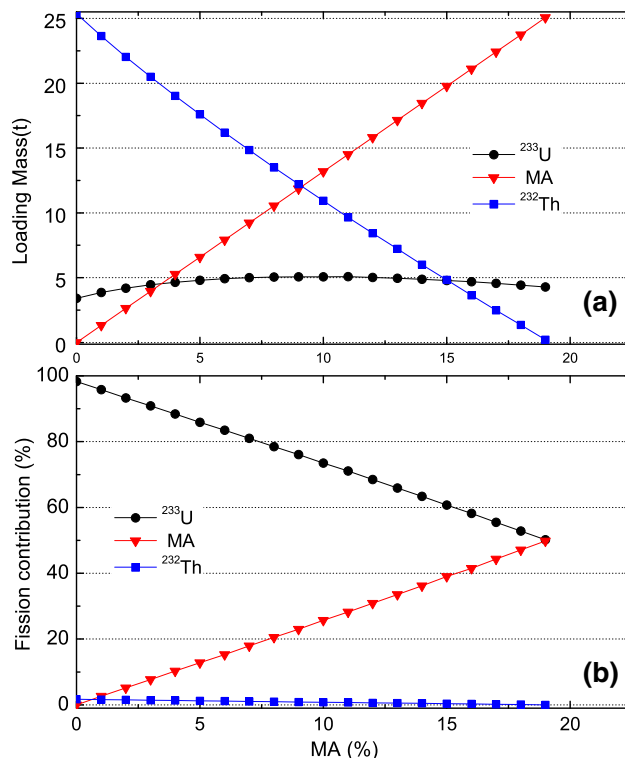
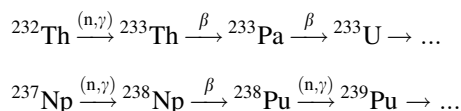


Fig. 5 Required initial actinides loadings and separate fission rate fractions of heavy nuclides as a function of MA fraction for $k_{\text{eff}} = 0.97$ (Color online)

the fission rate fraction of ^{233}U decreases from 98.35 to 50.21% and the contribution of the MAs to the fission reaction is nearly equal to the value of that of ^{233}U when the MA = 19.1%, resulting from the variation of the inventory of the actinides, as shown in Fig. 5a, while the spectrum hardening is shown in Fig. 6. The increasing MA inventory results in a harder spectrum, which can significantly reduce the mean cross section of the microscopic fission of ^{233}U ; however, it has a smaller effect on the fission cross section of MA. The contribution of MA rises nearly linearly with the increasing MA fraction. Compared with ^{232}Th which has a low fission rate fraction in all cases for its extremely small fission cross section, the MA have a non-negligible capability of neutron production with a higher instant reactivity.

The spectrum hardening resulting from the increasing MA loading can further affect the actinide neutronic performance, which can be assessed by using the concept of neutron depletion (ND). ND is defined as the neutron number required to transform a specific actinide nucleus including its capture and decay products into a final state (FPs). Its value indicates the neutron production or consumption of an actinide nucleus during an infinite operation cycle. For most MAs, at least two (n, γ) reactions are needed to be transformed into fissile fuel, while for a fertile fuel a single is needed, for example:



In a thermal reactor, for example in a PWR, the ND for most MAs is greater than zero. The MA transmutation in a thermal reactor can result in a remarkable neutron depletion. In contrast, a hard neutron spectrum can decrease α , shorten the reaction chain to fission, and reduce the neutron

depletion for actinides incineration. Table 2 shows the ND values of main actinides used in this study, and it can be seen that NDs of main actinides are less than zero, which indicates that these nuclei produce extra neutron as opposed to consume neutron during the total lifetime. In addition, the neutron production capacity of MAs, such as ^{237}Np and ^{241}Am can exceed that of ^{232}Th with the increasing MA fraction.

3.3 ^{233}U production and conversion ratio for MA loading

To assess the breeding capability of the ADS-MSR for different MA loadings with online fuel processing and refueling, burnup calculations were performed, while the net ^{233}U productions were calculated and extracted by using Eq. (3).

Figure 7a shows the net ^{233}U productions during the operation period for different MA loadings in the range of MA = 0–14%. It can be seen that MA loading has a significant effect on the evolution trends of the ^{233}U production. For MA = 1%, nearly no ^{233}U is produced or depleted in the first 5 years, then the ^{233}U production gradually increases similarly to the trend for MA = 0%. When the MA loading fraction reaches 4%, at the early stage of the operation (about the first 10 years), the reactor consumes a certain amount of ^{233}U and the ^{233}U depletion increases with the increasing MA loading fraction. Afterward, the reactor stops consuming ^{233}U and begins to breed additional ^{233}U with a production rate, which increases faster than that of MA < 1%. In summary, during the 50 years of operation, the increasing MA loadings (MA > 1%) in the ADS-MSR can lead to a higher net ^{233}U production, while a certain amount of ^{233}U is consumed in the first two decades, compared to the operation with MA < 1%.

Figure 7b shows the time evolution of the CR during the operation period. The evolution trends of the CR for different MA loadings are significantly different. The CR for a higher MA loading has an extremely low value at the beginning of the burnup and reaches the peak at the 20th year of the operation period. During the final 30 years, the CR gradually reduces until it became close to the value of

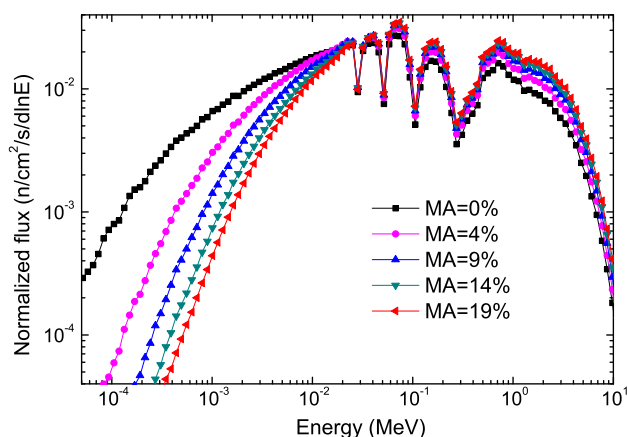


Fig. 6 Normalized neutron spectra for different MA loadings at the beginning of the burnup (Color online)

Table 2 Neutron depletion of actinides as a function of MA fraction

MA fraction (%)	^{232}Th	^{233}U	^{237}Np	^{241}Am
MA = 1	−0.212	−1.191	−0.139	−0.192
MA = 4	−0.256	−1.229	−0.341	−0.418
MA = 9	−0.303	−1.268	−0.523	−0.559
MA = 14	−0.334	−1.291	−0.627	−0.652

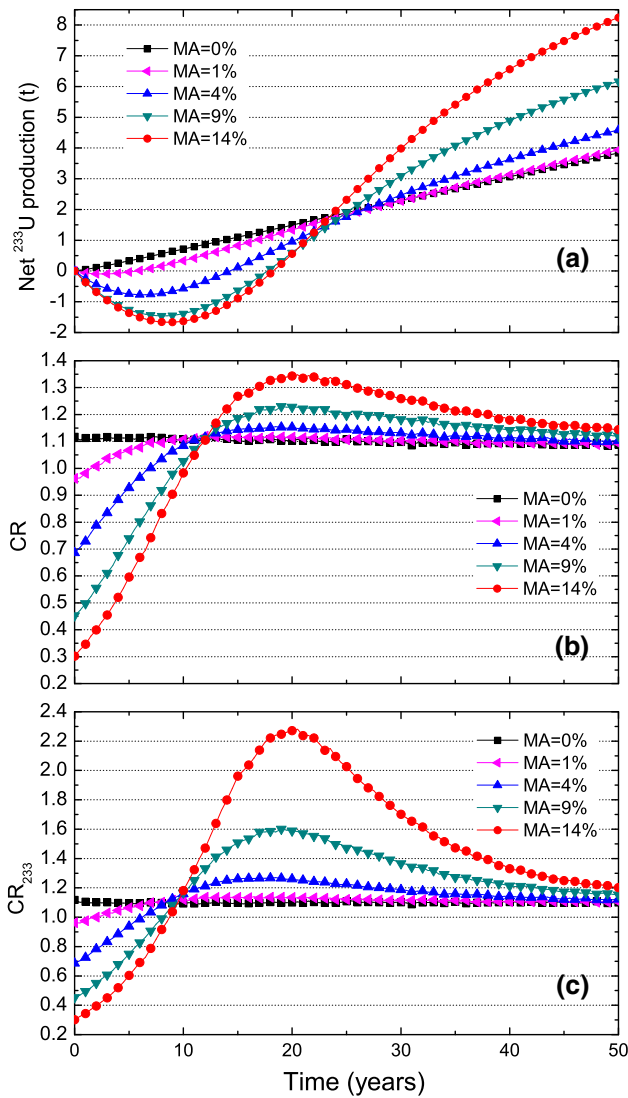


Fig. 7 Time evolution of **a** ^{233}U production, **b** CR, and **c** CR_{233} for different MA loadings ($k_{\text{eff}} = 0.97$) (Color online)

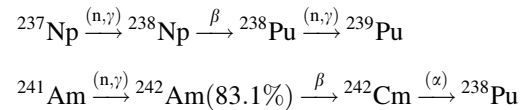
MA = 0%. However, the CR defined above, indicating the conversion performance of the whole fissile nuclides (^{233}U , ^{235}U , ^{239}Pu , and ^{241}Pu) in the core, is not unambiguous for the breeding analysis of ^{233}U . In order to describe the evolution trend of the ^{233}U breeding more accurately, a simplified CR can be defined as

$$\text{CR}_{233} = \frac{R_c(^{232}\text{Th} - ^{233}\text{Pa})}{R_a(^{233}\text{U})}, \tag{4}$$

where the R_c represents the capture reaction rate of ^{232}Th and ^{233}Pa while R_a denotes the absorption reaction rate of ^{233}U , while the other nuclides involved in Eq. (1) are not considered. Thus, CR_{233} is informative to show the evolution of ^{233}U in the reactor. The time evolution of CR_{233} is shown in Fig. 7c. It can be seen that CR_{233} is in good agreement with the trends of the ^{233}U net production shown

in Fig. 7a. When MA = 14%, in the 9th year, the reactor stops consuming ^{233}U , and the corresponding CR_{233} achieves one, while the CR is still less than one.

The variation of CR and CR_{233} depends on the evolutions of the inventory of the MAs and their daughter nuclides. In the first 9 years, CR_{233} is less than one resulting from the neutron capture of MA. As can be seen in Fig. 8, the Pu inventory increases rapidly and reaches a very high value during the earlier period. These generated Pu isotopes are primarily produced from neutron capture reactions from ^{237}Np and ^{241}Am , which are given by



These reactions consume a certain amount of neutrons, and as a result, the amount of neutrons is not sufficient for the ^{232}Th capture to breed ^{233}U . However, such Pu production results in a delayed contribution to fission reactions. During the final 40 years, most of the loading MA have been transformed into fissile nuclides and these fissile nuclides begin to provide surplus neutrons for more ^{233}U production than depletion. Thus, CR_{233} becomes much bigger than CR and then reaches a peak value. After 50 years of operation, nearly all the loading MA are burned with a higher net ^{233}U production, and then, the reactor returns to the operation mode of thorium–uranium fuel cycle.

The time evolution of ^{233}U fission fraction can also directly indicate the variation of reactivity during the entire operation cycle, as shown in Fig. 9. It can be seen, that for the high MA loading, ^{233}U is not the only contributor to the fission reaction. Especially when most of the MA were transmuted into fissile nuclides during approximately 10–20 years of operation, the ^{233}U fission fraction declines to a minimum value. The MA loading, together with its feature

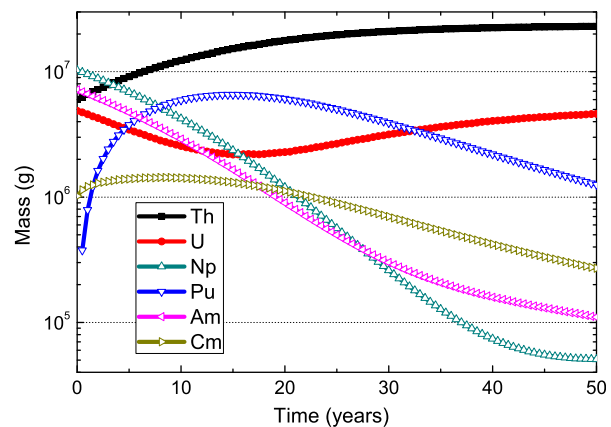


Fig. 8 Time evolution of actinides inventories for MA = 14% (Color online)

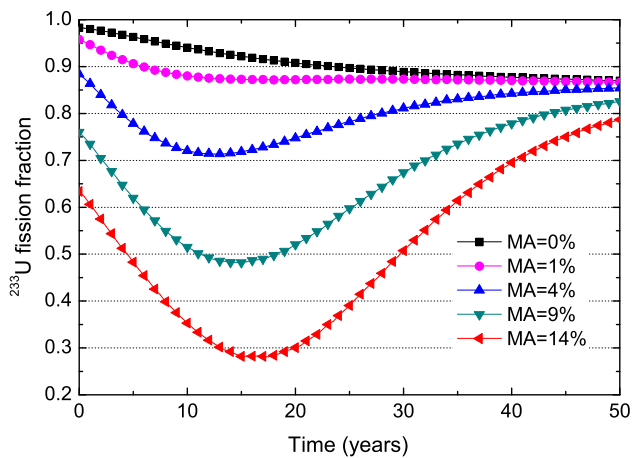


Fig. 9 Time evolution of ^{233}U fission fraction for different MA loadings (Color online)

of spectrum hardening, improves the immediate reactivity contribution to the core. Online refueling, which is important for a closed fuel cycle, provides a sufficiently long time of operation for the function of delayed reactivity from MA.

The calculation results above show the ^{233}U breeding capability in the subcritical molten salt reactor, when MA are loaded proportionally into the fuel salt. Meanwhile, the reactor has the additional ability of higher amount of MA transmutation than ^{233}U production. Figure 10 shows the MA fractional transmutations (FT) for different MA loadings calculated by

$$\text{FT}(t) = 1 - \frac{M(t)}{M_{\text{BOB}}}, \quad (5)$$

where $M(t)$ denotes the MA inventory at burnup time t and M_{BOB} is the MA inventory at the beginning of the burnup. When the MA fraction is very small ($\text{MA} = 0.1\%$), the FT

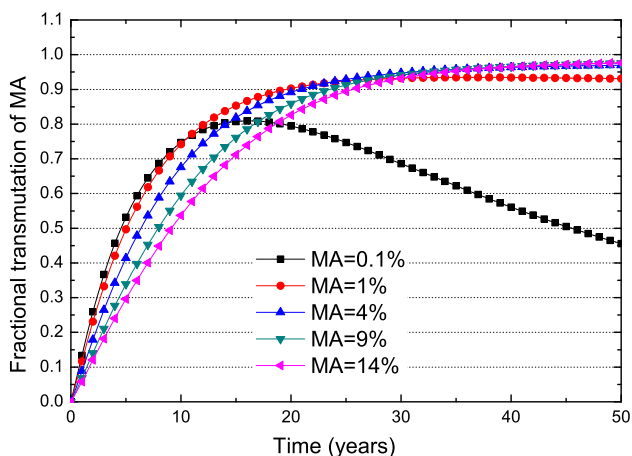


Fig. 10 Time evolution of MA fractional transmutation for different MA loadings (Color online)

of MA increases first and then declines, because the MA consumption is lower than the MA production during the final runtime. When $\text{MA} > 1$, the FT of MA can achieve 0.93–0.97 indicating that nearly all of the loading MA have been transmuted. It can also be seen that there is a correlation between the evolution trends of the MA fractional transmutations and the ^{233}U fission fraction trends shown in Fig. 9. In approximately 15 years, most of the MA has been burned or transformed into Pu and the ^{233}U fission fraction declines to its lowest value. In order to assess the transmutation capability more directly, the net mass of the MA transmutation needs to be calculated. The net MA transmutation mainly depends on the initial MA loading mass. For the different MA fractions of 1, 4, 9, and 14%, the net MA transmutation is approximately 1250, 5180, 11570, and 18020 kg, respectively.

4 Conclusion

In this study, the Th-U breeding capability of an ADS-MSR was assessed. The CR and the net ^{233}U production for various subcriticalities and different MA loadings were analyzed.

Results show that the subcriticality of the core has a considerable effect on the Th-U breeding of the ADS-MSR. The subcriticality characteristics can reduce the initial loading of ^{233}U and provide extra spallation neutrons, which can obviously enhance the CR, increase the net ^{233}U production, and reduce the doubling time. Specifically, the doubling time for k_{eff} of 0.99 is larger than 80 years, while the counterpart for k_{eff} of 0.93 is only approximately 22 years.

For the subcritical molten salt reactor with the MA loading fraction increasing from 0 to 19.1%, the initial ^{233}U loading first increases with the increasing MA fraction, reaching a peak value at about $\text{MA} = 9\%$, and then decreases. The fission rate fraction of ^{233}U decreases from 98.35 to 50.21% and the contribution of the MAs to the fission reaction is nearly equal to the value of ^{233}U when the $\text{MA} = 19.1\%$. In addition, the spectrum hardening resulting from the increase of the MA loading can further decrease the capture-to-fission ratio (α), shorten the reaction chain to fission, and reduce the neutron depletion for actinides incineration.

The MA loading also has a significant effect on the net ^{233}U production. For $\text{MA} > 1\%$, the evolution of the inventory of the MA and their daughter nuclides determine the trend of the CR. The MA capture a certain amount of neutrons and consume considerable ^{233}U in the first two decades, while the generated fissile nuclides result in a delayed contribution to fission reaction and increase the net

^{233}U production during the whole period of operation. For $\text{MA} = 1\%$, nearly no ^{233}U is produced or consumed in the first 5 years, while the ^{233}U production increases gradually similarly to $\text{MA} = 0\%$. In a subcritical reactor ($k_{\text{eff}} = 0.97$) with the MA fraction increasing from 1 to 14%, the net ^{233}U production increases from 3.94 to 8.24 t. Meanwhile, the reactor has an additional benefit that it burns a large amount of MA along with the ^{233}U production. When $\text{MA} > 1$, the fractional transmutation of MA can achieve 0.93–0.97 indicating that nearly all the loading MA at the beginning of the burnup have been transmuted.

References

1. P.A. Gokhale, S. Deokattey, V. Kumar, Accelerator driven systems (ADS) for energy production and waste transmutation: international trends in R&D. *Prog. Nucl. Energy* **48**, 91–102 (2006). <https://doi.org/10.1016/j.pnucene.2005.09.006>
2. H. Nifenecker, S. David, J.M. Loiseaux et al., Basics of accelerator driven subcritical reactors. *Nucl. Instrum. Methods Phys. Res. A* **463**, 428–467 (2001). [https://doi.org/10.1016/S0168-9002\(01\)00160-7](https://doi.org/10.1016/S0168-9002(01)00160-7)
3. W. Maschek, X. Chen, F. Delage et al., Accelerator driven systems for transmutation: fuel development, design and safety. *Prog. Nucl. Energy* **50**, 333–340 (2008). <https://doi.org/10.1016/j.pnucene.2007.11.066>
4. M.W. Rosenthal, P.R. Kasten, R.B. Briggs, Molten-salt reactors—history, status, and potential. *Nucl. Technol.* **8**, 107–117 (1970)
5. *Design Study of a Single-Fluid Molten-Salt Breeder Reactor. comp.* (Oak Ridge National Lab., Tenn, 1971). <https://doi.org/10.2172/4030941>
6. L. Mathieu, D. Heuer, A. Billebaud et al., in *Proposal for a Simplified Thorium Molten Salt Reactor*. Proceedings of GLOBAL (2005)
7. E. Merle-Lucotte, D. Heuer, C. Le Brun et al., in *Fast Thorium Molten Salt Reactors Started with Plutonium*. Proceedings of ICAPP'06. American Nuclear Society (2006), p. 6132-9
8. K. Furukawa, E.D. Greaves, L.B. Erbay et al., in *New Sustainable Secure Nuclear Industry Based on Thorium Molten-Salt Nuclear Energy Synergetics (THORiMS-NES)*. Nuclear Power-Deployment, Operation and Sustainability (2011), p. 407
9. K. Furukawa, Y. Kato, S.E. Chigrinov, Plutonium (TRU) transmutation and ^{233}U production by single-fluid type accelerator molten-salt breeder (AMSB). *AIP Conf. Proc.* **346**, 745 (1995). <https://doi.org/10.1063/1.491112>
10. I. Slessarev, V. Berthou, M. Salvatores et al., in *Concept of the Thorium Fuelled Accelerator Driven Subcritical System for Both Energy Production and TRU Incineration-'TASSE'* (1999)
11. C.D. Bowman, Once-through thermal-spectrum accelerator-driven light water reactor waste destruction without reprocessing. *Nucl. Technol.* **132**, 66–93 (2000). <https://doi.org/10.13182/NT00-1>
12. J. Vergnes, D. Lecarpentier, The AMSTER concept (actinides molten salt transmuter). *Nucl. Eng. Des.* **216**, 43–67 (2002)
13. A.M. Degtyarev, A.K. Kalugin, L.I. Ponomarev, Cascade subcritical molten salt reactor (CSMSR): main features and restrictions. *Prog. Nucl. Energy* **47**, 99–105 (2005). <https://doi.org/10.1016/j.pnucene.2005.05.008>
14. P.N. Alekseev, R.Y. Zakirov, V.V. Ignatiev et al., Concept of the cascade subcritical molten salt reactor (CSMSR) for harmonization of the nuclear fuel cycle. *Genshikaku Kenkyu* **43**, 5–15 (1999)
15. J.S. Hendricks, G.W. McKinney, M.L. Fensin, et al., Mcnpx 2.6.0 Extensions (Los Alamos National Laboratory, LA-UR-08-2216, 2008)
16. M.B. Chadwick, P. Oblozinsky, M. Herman et al., Endf/b-vii.0: next generation evaluated nuclear data library for nuclear science and technology. *Nucl. Data Sheets* **107**, 2931–3060 (2006). <https://doi.org/10.1016/j.nds.2006.11.001>
17. T. Mukaiyama, H. Yoshida, T. Ogawa, *Minor Actinide Transmutation in Fission Reactors and Fuel Cycle Considerations*. IAEA-TECDOC-693, vol. 86 (IAEA, Vienna, Austria, 1993)